

Indium Tin Oxide Based Wideband Dielectric Resonator Antenna for Wireless Communication

Vivek Parimi¹, Sajal Biring², Ku Chia Hao³, Abhirup Datta⁴, and Somaditya Sen^{5, 2, *}

Abstract—In this paper, a novel dielectric resonator antenna has been numerically simulated and experimentally demonstrated. The proposed design, comprising an Indium Tin Oxide (ITO) coated glass slide placed on a microstrip transmission line, is intended for WLAN and Wi-Max applications. The antenna shows a maximum bandwidth of 2.15–7.65 GHz and 10.36–11.78 GHz and a gain ranging from 2.21 to 6.44 dB. The novelty of the design lies in the use of ITO coating on the glass to enhance as well as regulate the antenna bandwidth. Parametric variations have been investigated to analyze the topology for understanding the effect of the design parameters on the gain, bandwidth, and reflection coefficient. A prototype has also been fabricated, where different ITO sheets have been mounted to measure the response. The proposed geometry has been found to be better and competent enough with respect to antenna parameters than existing Ultrawide Band antennas.

1. INTRODUCTION

Wireless Local Area Network (WLAN) has undergone rapid development in recent years [1]. WLAN (2.45 GHz) and WiMAX (5.8 GHz) [2] communications require cost and size efficient antennas with appropriate bandwidth for communication applications [3]. Ultrawide Band (UWB) Antenna is a type of antenna which has a large bandwidth and covers a large number of communication bands. Numerous UWB antennas exist today, such as planar, printed monopole/dipole, microstrip, dielectric resonator, wide-slot, and metamaterial antennas [4]. These designs tend to be large in size, difficult to manufacture, and expensive. Metamaterials involve a lot of complex fabrication issues and require sophisticated technology. Mono/dipole antennas are comparatively easier to construct but have low gain and narrow bands. Previously used patch antennas suffer from restricted bandwidths and are size inefficient [5]. Thus, as an alternative, Dielectric Resonator Antennas (DRAs) are investigated. Some of the advantages of DRAs include low cost, size efficiency, low conductive losses, high radiation efficiency, and flexible feed mechanisms [6]. Dielectric resonators have been used as frequency-specific filters in microwave circuits [7]. It soon gained importance as a radiating element, and by the early 1980s, the size efficiency potential and high-frequency applications created a new domain of research in DRAs [8]. Nowadays, DRA technology is a viable substitute for outdated and conservative antenna designs for wireless communications [9]. DRA materials generally involve intricate designs and setup. In previous research, studies have been conducted comparing the performance of various metals and ITO [10], and it was experimentally demonstrated that ITO had a superior response with respect to bandwidth, reflection coefficient, as well as gain. In this paper, a simple and inexpensive DRA, with considerable gain (G_R), notable bandwidth, and reflection coefficient (S_{11}), composed of a transmission line and an Indium Tin Oxide (ITO) coated glass slide [10], is proposed.

Received 16 July 2019, Accepted 12 January 2020, Scheduled 26 January 2020

* Corresponding author: Somaditya Sen (sens@iiti.ac.in).

¹ Department of Electrical Engineering, Indian Institute of Technology Indore, Indore 453552, India. ² Organic Electronics Research Center, Ming-Chi University of Technology, New Taipei 24301, Taiwan. ³ Department of Electrical Engineering, Ming Chi University of Technology, New Taipei 24301, Taiwan. ⁴ Discipline of Astronomy, Astrophysics and Space Engineering, Indian Institute of Technology Indore, Indore 453552, India. ⁵ Department of Physics, Indian Institute of Technology Indore, Indore 453552, India.

2. ANTENNA DESIGN

Figure 1 depicts the geometry of the DRA proposed in this work. A substrate made of FR-4 of length 50 mm (x -direction) and width 45 mm (y -direction) is chosen. The permittivity of the substrate was 4.3. The thickness of the substrate was 1.6 mm which is a standard industrial value. The microstrip transmission line was made of copper with dimensions of 3 mm \times 42 mm. The dimensions of the transmission line were selected to ensure an impedance of 50 Ω . The transmission line initiates at $x = 0$ and $y = 0$ as described in Fig. 1. The ground plane was made of copper and stretched along the width, W . It spreads over a length $g = 16$ mm along the L of the substrate.

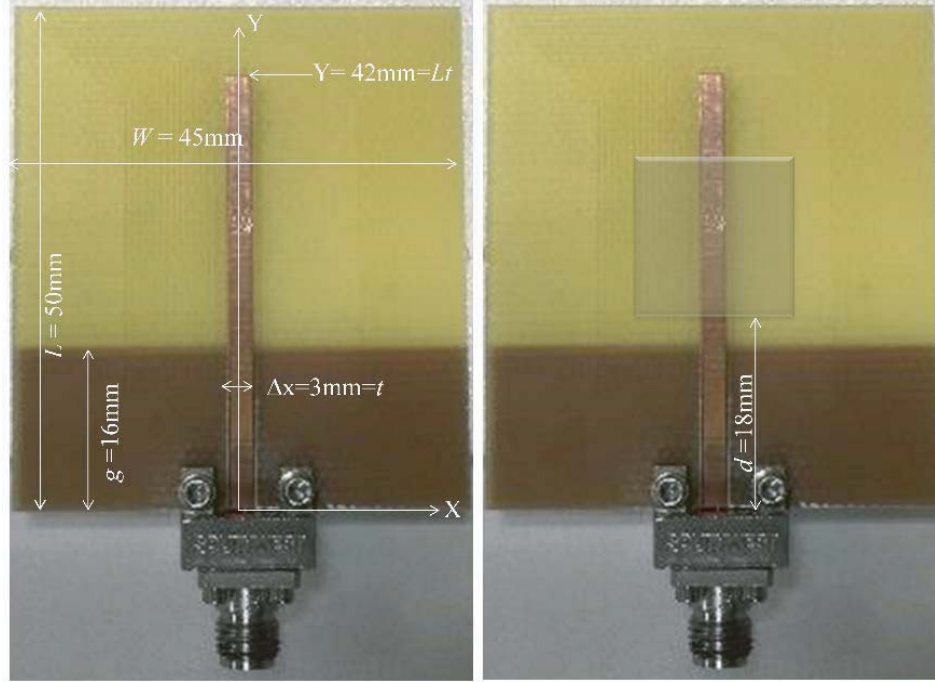


Figure 1. Model of the DRA depicting the components, configuration, and dimensions.

The ITO coated glass slides were placed directly on the transmission line at location $d = 18$ mm in the y direction ensuring physical contact between the two as shown in Fig. 1. The DRA was directly fed by the microstrip transmission line. The ITO coated glass slides used were cuboidal in shape with thickness 0.76 mm. The square ITO coated glass slides were of three different sizes: 10 mm \times 10 mm, 15 mm \times 15 mm, and 20 mm \times 20 mm. The permittivity of the glass was 4.82. The ITO layer had a resistivity of $7.2 \times 10^{-4} \Omega \text{ cm}$ and 90.2% transparency to visible light.

The DRAs had two different configurations. In one, the conducting ITO layer was the top surface. Hence, the transmission line and conducting ITO layer were separated by the glass layer. This setup is hereafter referred to as 10-t, 15-t, and 20-t for 10 mm \times 10 mm, 15 mm \times 15 mm, and 20 mm \times 20 mm slides, respectively. In the other configuration, the bottom surface of the slide contained the conducting ITO layer, and therefore, it was in contact with the microstrip transmission line. This setup is hereafter referred to as 10-b, 15-b, and 20-b for 10 mm \times 10 mm, 15 mm \times 15 mm, and 20 mm \times 20 mm slides, respectively.

The antenna was created using LPKF Protomat E33 PCB Fabricator. The design of the antenna was prepared on the LPKF fabricator software, and the milling instrument was used to cut the board into the desired shape accurately. The fabricator uses a high-speed drilling tool to cut away the copper layers wherever necessary to create the design of the antenna. A sharp cutting tool was then used to cut the antenna away from the board. After this, the board measurements were confirmed by using a digital Vernier caliper. The SMA connector was thereafter attached to the board.

3. SIMULATION TECHNIQUE

MicroWave Studio Suite (MWS) of Computer Simulation Technology (CST) software is used to analyze the performance of the designed antenna. The reflection coefficient, direction of radiation, etc. were determined using this software. The simulations are carried out using time-domain analysis in CST MWS. The model described above is created using the CST design tools. The DRA model is excited using a discrete port at one end of the transmission line. In order to improve simulation accuracy, materials with losses are used in the simulations. This ensures a much more accurate simulation result. Each simulation is carried out over a frequency range of 0–12 GHz. Within time-domain analysis, the Transmission Line Matrix (TLM) solver has been used. The TLM method provides an accurate broadband calculation and offers a very efficient octree-based meshing algorithm. This efficiently reduces the overall cell count. The scattering parameters were then collected and compared with the experimental values.

CST MICROWAVE STUDIO ® (CST MWS) is based on the finite integration technique (FIT), a very general approach, which describes Maxwell's equations on a grid space and can be written in time domain as well as in frequency domain and is not restricted to a certain grid type. A large step forward in the area of meshing was introduced by a method called "Perfect Boundary Approximation (PBA)", and it allowed a technique to represent curves and inclines very accurately within a coarse discretization. One main advantage of the time domain solver of CST MWS is that the resource requirement only scales linear with the number of mesh nodes and therefore the problem size. Thus it is possible to handle large radiating structures and even complete arrays with more than some hundreds of radiating elements. The ability to extract a high resolution of broadband antenna data is a result of the time domain solver's ability to define and calculate a large number of farfield monitors in one single simulation run. This represents a significant performance advantage compared to non-time domain methods which entail the simulation of a large number of discrete frequencies for the broadband data extraction. However, despite having the ability to solve a vast variety of problems, other techniques have shown advantages for certain class of problem. A frequency-domain method based on hexahedral and tetrahedral meshing was introduced to focus on the subset of problems where this technique excelled, e.g., in narrow band antennas, electrically small devices, or phased array unit cells. Both solvers — time and frequency domains — are completely available on a common user-interface.

4. EXPERIMENTAL SETUP

An Anritsu MS46122A 40 GHz Vector Network Analyzer (VNA) has been employed to measure the reflection coefficient (S_{11}) of the DRA. The data are recorded from the VNA using the Anritsu ShockLine software. The VNA is set up over a frequency spectrum of 0.01–12 GHz and is connected to the prototype with an SMA connector. S_{11} parameters are then obtained from the software and analyzed further.

5. RESULTS AND DISCUSSION

The transmission line displays responses at 2.15–2.59 GHz, 5.67–6.69 GHz, and 9.48–11.65 GHz [Fig. 2.] with considerable gain, G_R . G_R for the transmission line is mostly above 2 dB. However, one should note that the $|S_{11}|$ value is negligible, i.e., much less than a detectable strength (~ 10 dB) for most of the frequency range. When an ITO slide is introduced, the changes were drastic. Although G_R values did not vary much, the bandwidth improved considerably.

The responses of pure glass slides without ITO coating are an improvement from the transmission line. For the 10 mm \times 10 mm size, the bandwidths available for transmission are 2.15–2.54 GHz, 5.27–6.56 GHz, and 9.01–11.34 GHz. For the size of 15 mm \times 15 mm, the bandwidths available are 2.11–2.56 GHz, 5.15–6.23 GHz, 8.71–9.48 GHz, and 10.29–11.23 GHz. For the size of 20 mm \times 20 mm, the bandwidths available are 2.09–2.41 GHz, 5.12–6.13 GHz, 8.52–9.14 GHz, 10.31–11.27 GHz, 11.86 GHz and beyond. These responses are improved compared to the responses of the transmission line alone. However, these bandwidths are still limited and not appropriate for wideband communication purposes.

In the case of 10-b slide, the bandwidths available are 2.11–2.89 GHz, 4.82–7.01 GHz, 8.21 GHz, and higher. For 15-b slide, the bandwidths available are 2.20–3.44 GHz, 4.15–8.85 GHz, 10.14 GHz,

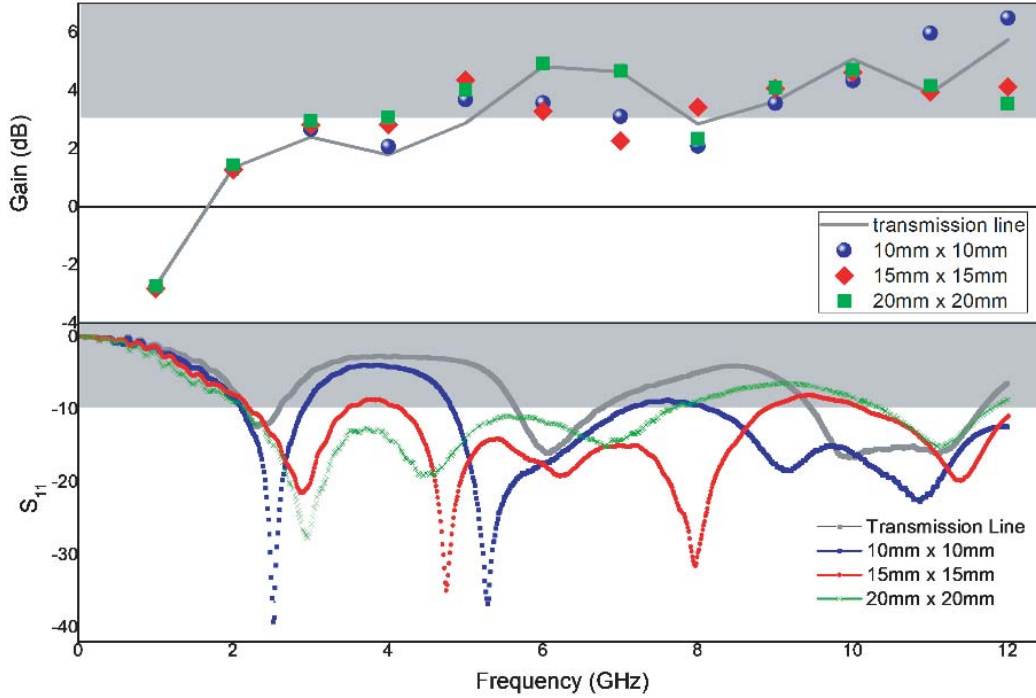


Figure 2. Measured values of the variation of gain and reflection coefficient (S_{11}) for transmission line and bottom ITO coated glass slides of the three dimensions with frequency.

and higher, whereas for 20-b slide, these available bandwidths are 2.14–7.66 GHz and 10.37–11.79 GHz. Hence, the bandwidth increases with an increase of dimensions of the DRA, thereby converting a low bandwidth device to a high bandwidth device.

Similarly, the results of 10-t, 15-t, and 20-t are analogous to 10-b, 15-b, and 20-b. For 10-t slide, the bandwidths available are 2.15–2.76 GHz, 4.99–6.35 GHz, and 8.47–12.02 GHz. For 15-t slide, these bandwidths are 1.99–2.86 GHz, 4.46–5.32 GHz, 5.74–9.02 GHz, and 9.98–11.84 GHz. For 20-t slide, these bandwidths are 1.69–3.02 GHz, 3.75–5.01 GHz, 5.82–7.58 GHz, and 10.21–11.70 GHz. Note that although the bandwidths have improved, the responses of 10-t, 15-t, and 20-t are not as strong as 10-b, 15-b, and 20-b.

The frequency responses of ITO coated glass slides are an improvement from the transmission line as well as pure glass slides. The bandwidths are wider and cover WLAN (2.4–2.5 GHz), WiMAX (5.15–5.85 GHz) and some 4G communication bands.

Figures 3 and 4 demonstrate the antenna performance when ITO coated glass slides are used as compared to pure glass slides and the transmission line. There is an enhancement in bandwidth as well as in S_{11} . This makes the use of these slides ideal for wideband communication applications. It is also observed that there is a shift in the frequency of maximum $|S_{11}|$. Thus, by using ITO coated glass slides, we can modify the characteristics of the transmission line to work in various frequency ranges.

The S_{11} spectrum is composed of certain frequencies where the antenna has maximum transmission. An inverse peak fitting has been performed on the frequency dependent S_{11} values. The frequencies of maximum $|S_{11}|$ for the transmission line are 2.36, 6.03, 6.68, 9.93, and 11.08 GHz, with $|S_{11}|$ ranging from 6 to 13 dB. The low $|S_{11}|$ values of these responses lead to narrow bandwidths. With the introduction of ITO coated glass slides, these responses are enhanced (higher values of $|S_{11}|$), and there is a shift in the position of the frequency of maximum $|S_{11}|$ as shown in Fig. 5.

The increase in bandwidth is a result of these changes. Note that these shifts are insignificant in the cases of 10-b and 10-t slides. These shifts are much more significant in 15-b and 15-t slides and most significant in 20-b and 20-t slides. We observe that the resonant frequencies of the transmission line around 6 GHz and 9 GHz come closer and eventually merge as we increase the size of the ITO coated glass slide samples. A similar observation can be made for the resonant frequencies of the transmission

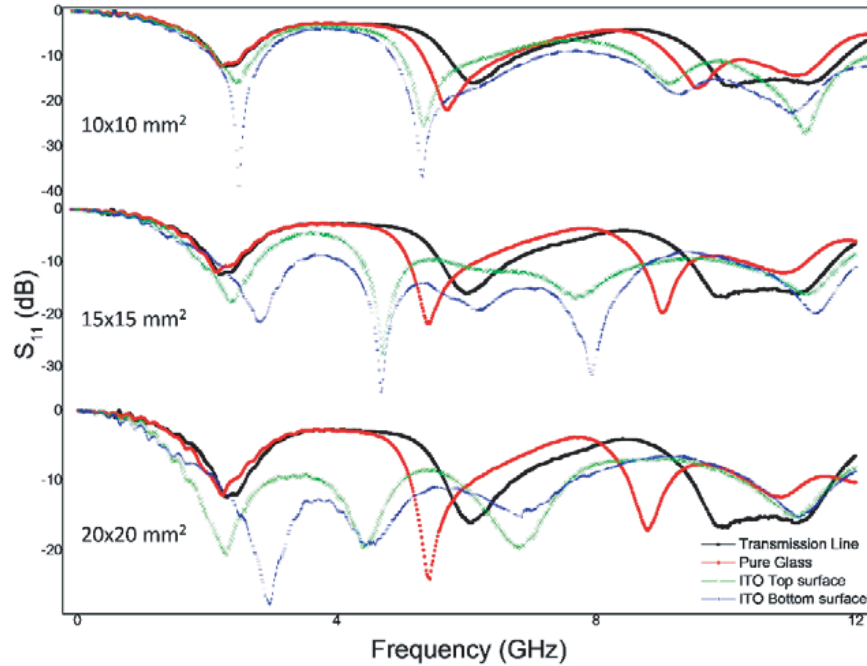


Figure 3. Comparison of S_{11} of the transmission line, and a pure glass slide, ITO top coated slides and ITO bottom coated slides of dimension $10 \times 10 \text{ mm}^2$ and $15 \times 15 \text{ mm}^2$ and $20 \times 20 \text{ mm}^2$ slide.

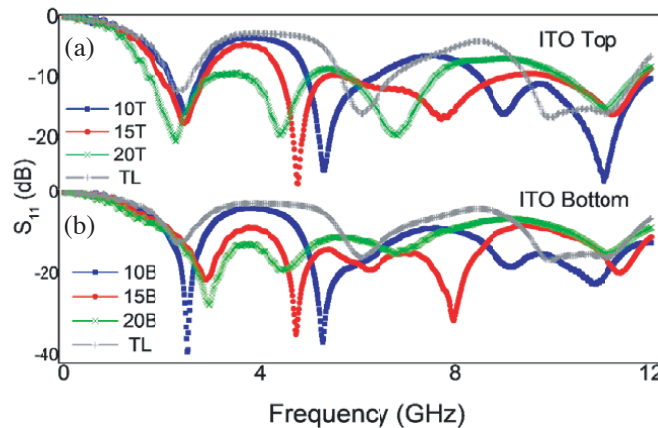


Figure 4. Measured reflection coefficients (S_{11}), of the DRA with ITO slides of sizes $10 \times 10 \text{ mm}^2$, $15 \times 15 \text{ mm}^2$ and $20 \times 20 \text{ mm}^2$ with (a) ITO layer bottom and (b) ITO layer top.

line around 2 GHz and 4 GHz; however, the bands do not merge.

The behavior of the ITO coated glass slide seems very similar to that of a rectangular patch antenna but with the advantage of lower losses since it has a lower conductivity which reduces the effect of metallic losses that would occur due to copper or other metal-based patches. Fig. 6 shows the simulated and measured $|S_{11}|$ of the 10-b, 15-b, and 20-b samples. The simulated and measured values closely match with each other. The simulated results of 10-b and 20-b are very similar to the measured values. In the case of 15-b, there is a slight shift of some of the modes; however, the bandwidths in simulated and measured responses in WLAN and WiMAX bands are accurate.

The far-field radiation patterns simulated in CST are plotted. The direction of the main lobes seems highly dependent on the frequency as shown in Fig. 7.

For 10-b slides, gain (G_R) of the antenna is significantly greater than 3 dB and lies between 2.21

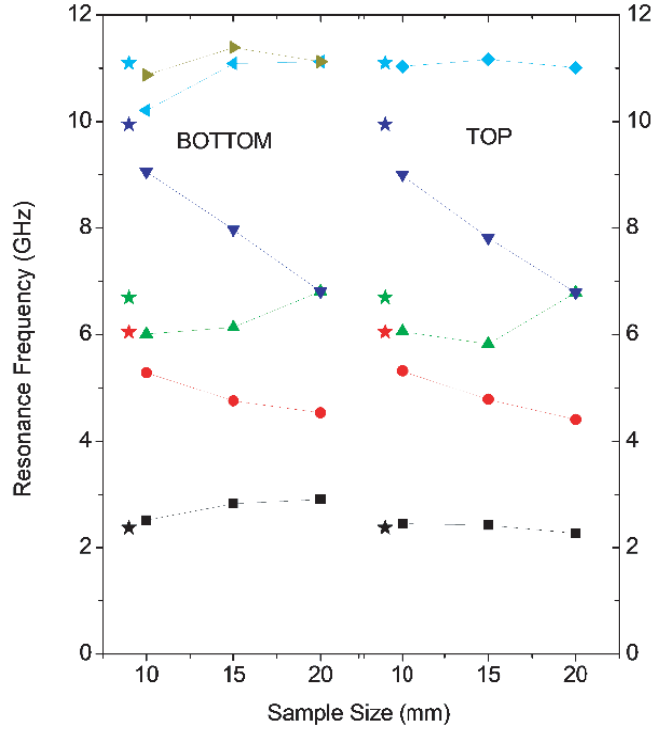


Figure 5. Variation of the resonance frequency (frequency of minima in the S_{11} graph) with the size of the glass slide. The star denotes the resonance frequency of the transmission line and the points depict the frequency of resonance of the ITO coated glass slides.

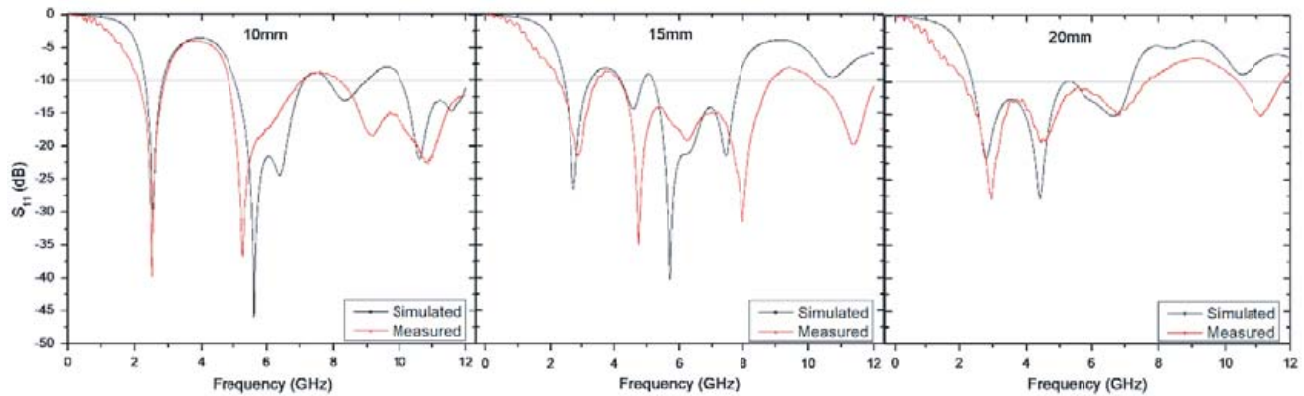


Figure 6. Comparison of simulated and measured S_{11} of the 10-b, 15-b and 20-b configurations.

and 6.44 dB. This makes it appropriate for communication purposes. For 10-t slide, the gain is very similar to 10-b. For 15-b slides, the gain is marginally reduced compared to 10-b slide and lies between 2.37 and 4.35 dB. The 15-b slide is applicable to lower frequency ranges than 10-b slide because its bandwidth lies in a lower frequency range. 15-t and 15-b slides have comparable gain values. For 20-b slides, the antenna gain in the frequency bands of transmission lies between 2.95 and 4.7 dB. This reveals the largest bandwidth and gain which is similar to the gains of 15-b and 10-b slides. Like the smaller sized slides, 20-t and 20-b slides also display comparable gains.

This work reports gains ranging from 2.21 to 6.44 dB in the frequency range 2.15–7.65 GHz and 10.36–11.78 GHz. A comparison with current models of UWB antennas shows that the average gain for any antenna in the range of 3–10.6 GHz can range from 2 to 6 dB. A patch antenna [10] records

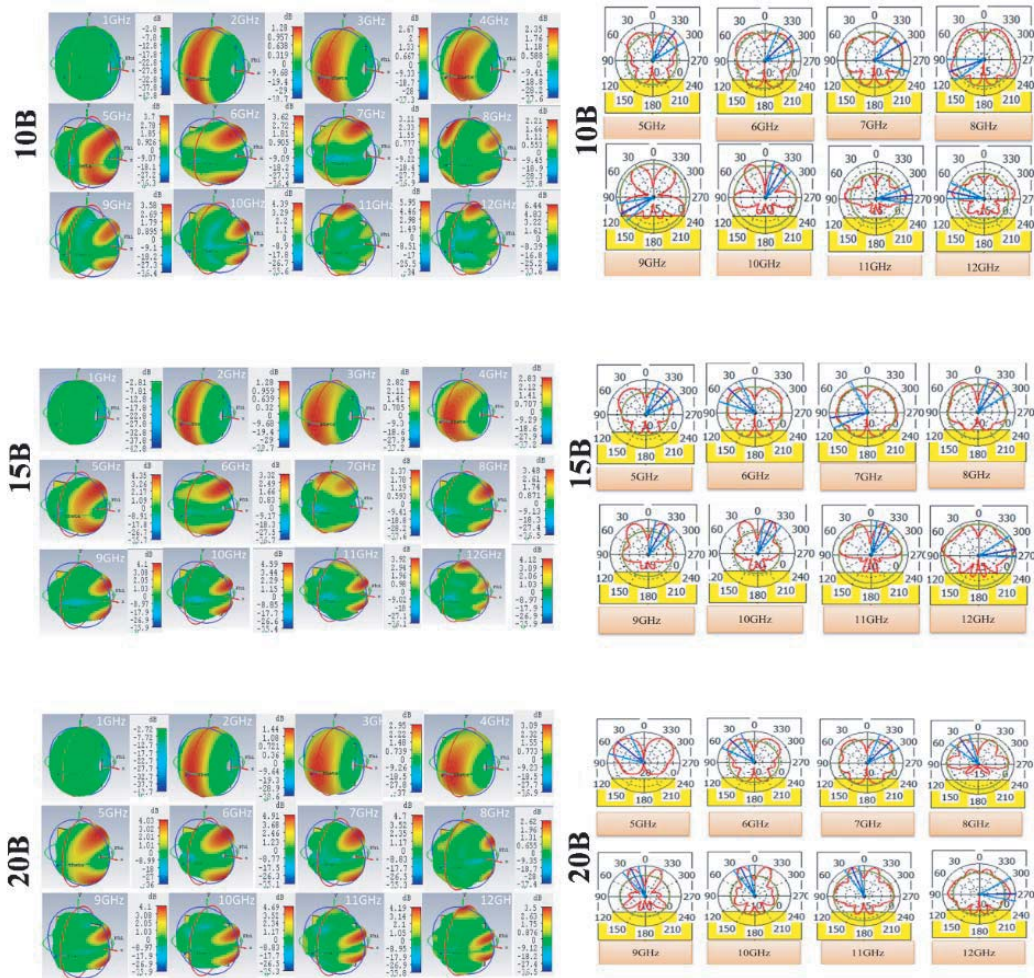


Figure 7. Far field patterns of 10-b, 15-b, 20-b configurations over 1–12 GHz and far field cuts over 5–12 GHz.

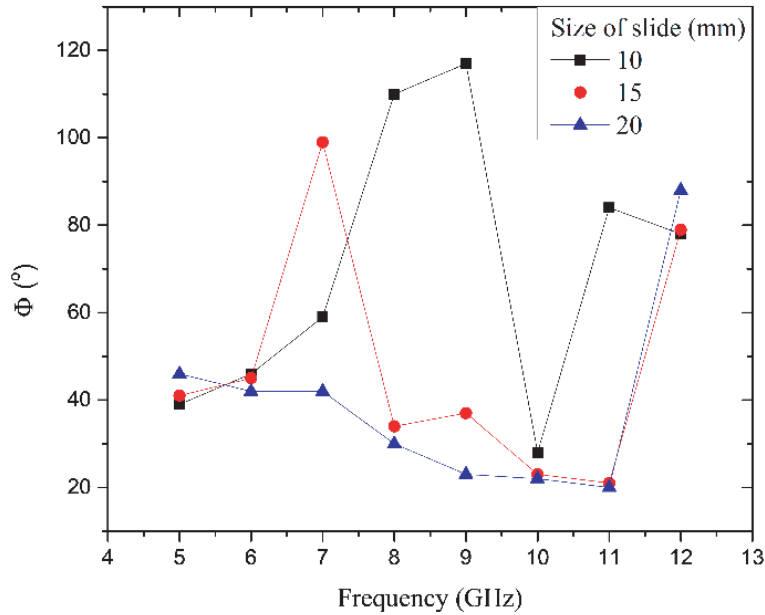
a peak gain of 2.45 dB. A curved Newton egg monopole antenna [11] works in a frequency range of 3.1–10.6 GHz with a gain ranging from 2.2 to 2.9 dB. A notched planar antenna [12] shows an average gain of 3.62 dB and bandwidth of 2.9–11 GHz. In the case of a metamaterial UWB antenna based on resonators (SRR) [13], the measured gain (G_R) exhibits a maximum gain of 8.57 dB at 13.5 GHz and a minimum gain of 2.71 dB at 18.6 GHz, with an average gain of 5.62 dB over the working frequency bands (3.07–19.91 GHz). An H-shaped metamaterial antenna [14] revealed G_R to be in the range of 2–6.8 dB in only a specific low-frequency range 1.2–6.7 GHz. The most interesting high gain UWB antenna is the Compact MTM UWB antenna [15] which operates in the range 3.07–19.91 GHz with an average gain of 5.62 dB. A compact DRA design [16] has a bandwidth of 3.1–10.6 GHz with an average of 5 dB. A mushroom-shaped DRA with a reflector shows an average gain of 14 dB over a frequency bandwidth of 4.7–9.2 GHz. G_R of some antennas used for UWB applications are shown in Table 1.

The radiation direction varies with frequency. It is interesting to note that the number of lobes of maximum intensity of radiation varies with the number of $|S_{11}|$ maxima below the frequency of interest. At lower frequencies which are below 4 GHz, the radiation pattern resembles that of a monopole antenna radiating along the z -axis direction. At higher frequencies above 4 GHz, the radiation is due to the higher-order resonant modes, which result in the splitting of the radiation lobe. From frequencies 5–12 GHz, the radiation is primarily in the XY -plane. There are multiple radiating lobes at these higher modes. The direction of maximum radiation intensity (ϕ) varies from 20° to 120° as shown in Fig. 8.

Hence, by using an unsophisticated antenna model constituted of a transmission line and ITO

Table 1. Comparison of ITO coated glass DRA with UWB antennas.

Antenna Type	Frequency Band (GHz)	Gain (dB)
U-shaped patch antenna [11]	4.7–11.1	2.45
Curved monopole antenna (Newton egg) [12]	3.1–10.6	2.2–2.9
Notched planar antenna [13]	2.9–11	3.62
MTM antenna (SRR) [14]	2.9–9.9	–1–5
H shaped cell based MTM antenna [15]	1.2–6.7	2–6.8
Compact MTM UWB antenna [16]	3.07–19.91	5.62
Compact DRA UWB design [17]	3.1–10.6	5
Mushroom shaped DRA with reflector [18]	4.7–9.2	14
ITO coated glass-based DRA	2.2–12	2.21–6.44

**Figure 8.** Variation of radiation direction maxima, ϕ ($^{\circ}$) in the XY -plane from 5–12 GHz frequency range.

coated glass slides, a competent DRA antenna with considerable gain and large bandwidth can be fabricated for communication applications.

6. CONCLUSION

A novel model of an ITO coated glass slide placed on a transmission line behaves as an excellent antenna with a wide bandwidth with frequency bands ranging from 2.2 to 12 GHz and gain ranging from 2.21 to 6.44 dB. This antenna model uses a commonly produced material ITO, which could help produce inexpensive antennas for communication applications. Size variation of the ITO coated glass slides and antenna performance is investigated, and it is shown that a larger ITO coated glass DRA (20 mm) performs better than smaller ITO coated glass DRAs (10 mm and 15 mm). It is also observed that if the conducting ITO layer is in direct contact with the transmission line, the bandwidth and reflection coefficient are better than having glass in contact with the transmission line. The model proposed is found similar to a metal patch antenna with advantages of low metallic losses. The model is shown to

be applicable in the dual bands of WLAN and WiMAX. The variation of the direction of radiation of the antenna with frequency was analyzed by observing the far-field patterns and cuts of simulations, which showed us the direction of radiation at various frequency modes. A comparison of this model was made with UWB antennas of other prevalent technologies, and it was observed that this model is an easy and inexpensive solution yielding comparable and sometimes better gain and bandwidth.

ACKNOWLEDGMENT

The principle investigator expresses sincere thanks to the Ming-Chi University of Technology, Taiwan for funding the research. The first author sincerely thanks MCUT for funding the travel, accommodation, and scholarship for a two and a half months summer internship during May–July 2018, during which this work was entirely completed at MCUT. The first author also thanks IIT Indore for allowing this internship to materialize as part of its curriculum. One of the authors (Dr. Sajal Biring) acknowledges financial support from the Ministry of Science and Technology (Grant Nos. MOST 106-2221-E-131-027 and 107-2221-E-131-029-MY2).

REFERENCES

- Holt, K., “Wireless LAN: Past, present, and future,” *Proc. DATE*, 2005.
- Nuaymi, L., “WiMAX: Technology for broadband wireless access,” [Online], Available: <https://onlinelibrary.wiley.com/doi/pdf/10.1002/9780470319055>, May 2007.
- Chen, Z. N., X. Qing, T. S. P. See, and W. K. Toh, “Antennas for WiFi connectivity,” *Proc. IEEE*, 2322–2329, 2012.
- Cicchetti, R., E. Miozzi, and O. Testa, “Wideband and UWB antennas for wireless applications: A comprehensive review,” *International Journal of Antennas and Propagation*, 1–45, [Online], Available: <https://doi.org/10.1155/2017/2390808>, February 2017.
- Liu, Y., L.-M. Si, M. Wei, P. Yan, P. Yang, H. Lu, C. Zheng, Y. Yuan, J. Mou, X. Lv, and H. Sun, “Some recent developments of microstrip antenna,” *International Journal of Antennas and Propagation*, 1–10, [Online], Available: <http://dx.doi.org/10.1155/2012/428284>, January 2012.
- Soren, D., R. Ghatak, R. K. Mishra, and D. R. Poddar, “Dielectric resonator antennas: Designs and advances,” *Progress In Electromagnetics Research B*, Vol. 60, 195–213, 2014.
- Lim, E. H. and K. W. Leung, “Use of the dielectric resonator antenna as a filter element,” *IEEE Transactions on Antennas and Propagation*, Vol. 56, No. 1, 5–10, 2008, [Online], Available: https://www.researchgate.net/publication/3019516_Use_of_the_Dielectric_Resonator_Antenna_as_a_Filter_Element
- Leung, K. W., K. M. Luk, K. Y. A. Lai, and D. Lin, “Theory and experiment of a coaxial probe fed hemispherical dielectric resonator antenna,” *IEEE Transactions on Antennas and Propagation*, Vol. 41, No. 10, 1390–1398, October 1993, [Online], Available: <http://dx.doi.org/10.1155/2016/6075680>.
- Petosa, A., A. Ittipiboon, and M. Cuhaci, “Dielectric resonator antenna technology for wireless applications,” *1998 IEEE-APS CAPWC*, 117–120, 1998.
- Parimi, V. M., A. Datta, S. Biring, C. H. Ku, and S. Sen, “Simple dielectric resonator antennas using ITO, Al and Ag coated glass on a transmission line,” *AIP Conference Proceedings 2100*, 020097, April 2019, Available: <https://doi.org/10.1063/1.5098651>.
- Mandal, K. and P. P. Sarkar, “High gain wide-band U-shaped patch antennas with modified ground planes,” *IEEE Transactions on Antennas and Propagation*, Vol. 61, No. 4, 2279–2282, April 2013, [Online], Available: http://www.academia.edu/30138505/High_Gain_Wide-Band_U-Shaped_Patch_Antennas_With_Modified_Ground_Planes.
- Verma, S. and P. Kumar, “Printed Newton’s egg curved monopole antenna for ultrawideband applications,” *IET Microwaves, Antennas & Propagation*, Vol. 8, No. 4, 278–286, November 2013, [Online], Available: <https://digital-library.theiet.org/content/journals/10.1049/iet-map.2013.0144>.

13. Islam, M. T., R. Azim, and A. T. Mobashsher, "Triple band-notched planar UWB antenna using parasitic strips," *Progress In Electromagnetics Research*, Vol. 129, 161–179, June 2012.
14. Rani, M. S. A., S. K. A. Rahim, M. R. Kamarudin, T. Peter, S. W. Cheung, and B. M. Saad, "Electromagnetic behaviors of thin film CPW-fed CSRR loaded on UWB transparent antenna," *IEEE Transactions on Antennas and Propagation*, Vol. 13, 1239–1242, July 2014, [Online], Available: <https://doi.org/10.1109/LAWP.2014.2332514>.
15. Alibakhshi-Kenari, M., M. Naser-Moghadasi, R. A. Sadeghzadeh, and B. S. Virdee, "Metamaterial-based antennas for integration in UWB transceivers and portable microwave handsets," *International Journal of RF and Microwave Computer-Aided Engineering*, Vol. 26, No. 1, 88–96, September 2015, [Online], Available: <https://onlinelibrary.wiley.com/doi/abs/10.1002/mmce.20942>.
16. Islam, M. M., M. T. Islam, M. Samsuzzaman, and M. R. I. Faruque, "Compact metamaterial antenna for UWB applications," *Electronics Letters*, Vol. 51, No. 16, 1222–1224, August 2015, [Online], Available: <https://ukm.pure.elsevier.com/en/publications/compact-metamaterial-antenna-for-uwb-applications>.
17. Ge, Y., K. P. Esselle, and T. S. Bird, "Compact dielectric resonator antennas with ultrawide 60%–110% bandwidth," *IEEE Transactions on Antennas and Propagation*, Vol. 59, No. 9, 3445–3448, July 2011, [Online], Available: <https://doi.org/10.1109/TAP.2011.2161538>.
18. Cicchetti, R., A. Faraon, E. Miozzi, R. Ravanelli, and O. Testa, "A high-gain mushroom-shaped dielectric resonator antenna for wideband wireless applications," *IEEE Transactions on Antennas and Propagation*, Vol. 64, No. 7, 2848–2861, April 2016, [Online], Available: <https://ieeexplore.ieee.org/document/7463018>.